Noname manuscript No.
(will be inserted by the editor)

Ultrasensitivity in Independent Multisite Systems

Shane Ryerson · German A. Enciso

Received: date / Accepted: date

Abstract Multisite modifications are widely recognized as an essential feature of many switch-like responses in signal transduction. It is usually assumed that the modification of one site directly or indirectly increases the rate of modification of neighboring sites. In this paper we provide a new set of assumptions for a multisite system to become highly ultrasensitive even in the absence of cooperativity or allostery. We assume that the individual sites are modified independently of each other, and that protein activity is an ultrasensitive function of the fraction of modified sites. These assumptions are particularly useful in the context of multisite systems with a large (8+) number of sites. We estimate the apparent Hill coefficient of the dose responses in the sequential and nonsequential cases, highlight their different qualitative properties, and discuss a formula to approximate dose responses in the nonsequential case. As an example we describe a model of bacterial chemotaxis that features robust ultrasensitivity and perfect adaptation over a wide range of ligand concentrations, based on non-allosteric multisite behavior at the level of receptors and flagella. We also include a model of the inactivation of the yeast pheromone protein Ste5 by cell cycle proteins.

Keywords Multisite system · Phosphorylation · Signal transduction · Ultrasensitivity · Cooperativity · Allostery · Bacterial chemotaxis

MSC Classification: 92C40, 92C42, 37N25

G.A. Enciso (Corresponding Author)
Mathematics Department
University of California, Irvine (USA)
Tel.: +1 949 824 3727
E-mail: enciso@uci.edu

S. Ryerson
Mathematics Department
University of California, Irvine (USA)

1 Introduction

Multisite proteins have long been used as a framework to create all-or-none responses involved in many cellular decision-making processes. In the well known 1965 work by Monod, Wyman, and Changeux [29], the allosteric behavior of the hemoglobin protein was proposed as a source of such ultrasensitive responses. Cooperativity and allostery have been widely studied and modeled ever since, and they rightly deserve this attention given the large number of enzymes and other proteins that use this mechanism or the related one proposed by Koshland, Némethy, and Filmer [23]. In fact, interest in the paper [29] has increased substantially in recent years, with up to 200 citations per year in 2012 according to Google Scholar.

In the current paper we explore a simple mechanism for ultrasensitive behavior in multisite biochemical systems. However the conceptual assumptions will be quite different to those made for allosteric and cooperative models. Instead of assuming that the modification of one site facilitates the modification of neighboring sites (the standard definition of cooperativity, see also Ferrell [12]), we assume that all sites are modified independently of each other. We also assume that all sites contribute equally to protein activation, for instance by changing the broad electrostatic properties of the protein in the case of phosphorylation. Thus the different sites only 'cooperate' with each other at the level of protein activation, not at the level of site modification.

This set of assumptions nicely complements the large body of existing work for cooperative systems. Cooperativity usually arises from allostery, whereby the different sites of a protein affect each other through internal structural interactions. Allostery implicitly imposes certain restrictions on the structure of the system. For instance, it is unlikely that a protein with multiple phosphorylation sites in an unstructured domain would observe allostery. Yet there is evidence that multisite phosphorylation is most common in such unstructured domains [21]. There are many other multisite modifications other than phosphorylation that could fit into this framework. These include acetylation, methylation, ligands binding to receptor complexes, transcription factors binding to multisite promoter regions, histones binding to DNA, among many others. The assumption of independence between sites allows to estimate the probability of a protein being in a given state in terms of the individual probabilities at each site. In effect, this reduces the dynamics of protein activation to determining the dynamics of single site modification, as will be shown below in detail.

We define $a(x)$ as the fractional activity of a molecule having a fraction x of modified sites. So for example, if a substrate has multiple phosphorylation sites and it must be bound to the membrane to be active, then $a(0.2)$ is the fraction of time the molecule is bound when 20% of its sites are phosphorylated. Under many different scenarios, $a(x)$ can potentially be shown to be an ultrasensitive function - see for instance bulk electrostatic systems [36], or the elegant entropy-based mechanism developed in [24]. We discuss in particular a

derivation in Section 6 showing that $a(x)$ can become arbitrarily ultrasensitive for increasing values of n.

Under the given assumptions we derive the formula

$$f(E) \approx S_{tot} a(z(E)), \tag{1}$$

where $f(E)$ is the dose response and $z(E)$ is the fraction of modified sites in the sample given an input E, and S_{tot} is the total substrate concentration. This formula becomes increasingly precise as the number of sites n grows. The dose response can therefore be ultrasensitive for large n to the extent that $a(x)$ itself is an ultrasensitive function. This is an equation of predictive value because it relates different quantities of the system that can be independently measured in the lab. Also, as it will become clear with the examples, this formula fully takes into account the large number of sites without introducing numerous additional variables. It can be used as a modeling technique to resolve a common problem in many multisite models, which either have a large number of very similar variables or else tend to trivialize the complexity of the system by effectively assuming that there is only one site.

Multisite systems can be modeled using sequential or nonsequential mechanisms. In sequential models, the protein sites are modified in a specific order. Nonsequential models do not assume this, which is more realistic but has the disadvantage of greatly increasing the number of protein states. We show through analysis and simulations that sequential systems can become ultrasensitive even if the fractional activity function $a(x)$ itself is not ultrasensitive. In fact, the apparent Hill coefficient is estimated to be proportional to $n+1$, so that the ultrasensitivity increases arbitrarily with n. This shows one possible mechanism that a biological system could use to become highly ultrasensitive, by ensuring a sequential modification framework.

We provide concrete examples in the context of well known biological models. Our main example is a compact model of bacterial chemotaxis that is sensitive to small differences in chemoattractant concentration due to multisite effects. Chemoattractant ligands bind to receptors that are known to form highly structured hexagonal arrays [17]. If the interaction among receptors creates an ultrasensitive fractional activity function, then the system can be highly sensitive to small short term increases in ligand concentration, even if the ligand binding events are largely independent of each other. This model also features perfect adaptation to long term chemoattractant concentration levels through an integral feedback mechanism. The ultrasensitivity and adaptation hold over a wide range of ligand concentrations and also for large ranges of parameter values provided that a simple calibration equation is satisfied. At the level of the flagellar motor, the downstream chemotaxis signaling molecule CheY binds to one of around 40 different sites near the motor to determine the bias for clockwise or counterclockwise rotation [9], through a mechanism that is not yet well understood. Once again, assuming that the motor bias is an ultrasensitive function of the fraction of bound CheY ligands (e.g. through the general mechanism described in detail in Section 6), one can show a high

sensitivity in motor bias to small changes in CheY concentration. This holds even if the binding of CheY to the flagellum is not cooperative.

Another example involves the yeast pheromone pathway, which becomes inactive during the cell cycle through multisite phosphorylation of the scaffold protein Ste5 by the cell cycle regulator Cdk1. Based on a model by Serber and Ferrell [36], we show how this inactivation can become ultrasensitive under proper circumstances even if there is no cooperativity in the phosphorylation.

It should be stressed that there are other mechanisms in the literature modeling ultrasensitivity under similar conditions, albeit relying on different assumptions. One of the most common systems is the zero-order mechanism, introduced by Goldbeter and Koshland [14], which operates under a saturation regime even in the presence of a single modification site. Goldbeter and Koshland also considered the synergy between zero-order and multistep interactions in [15], and they found that they can complement each other. In the current manuscript we do not assume that the substrate concentrations lie in the saturation regime, but rather that the substrates are far from saturation and enzyme reaction rates are approximately linear. Sequential multisite models of ultrasensitivity are common in the literature and are generally derived using specific assumptions such as increasing the reaction rates of the last few modifications [16] or by the use of protein relocalization [11,26]. Gunawardena showed in [16] that the standard sequential model is actually not very ultrasensitive by itself. Other forms of ultrasensitivity include signaling cascades [20,32] and allovalency [25]. For many more references, see the recent review by the senior author on mechanisms for ultrasensitive behavior [10].

2 Ultrasensitivity in nonsequential systems

We start with a short mathematical analysis of a nonsequential multisite system, showing how dose responses can be approximated using the fractional activity function $a(x)$. This approximation becomes increasingly precise as the number of sites increases. If $a(x)$ is ultrasensitive, then this property can be transferred to the dose response. Suppose that a protein substrate S has n modification sites, which can represent multisite phosphorylation, multisite ligand binding, etc. There is a total of 2^n possible states for the protein, and each of the sites is modified at a rate proportional to the concentration of the input E, which could be e.g. an enzyme or a ligand. The modifications are removed at a rate proportional to the concentration of a protein F (e.g. a phosphatase). The modifications are nonsequential, i.e. they are attached and removed in no particular order (Figure 1a). The modification and demodification reactions are each considered to be irreversible, and depending on the biochemical context they can represent covalent or non-covalent modifications. In order to simplify the dynamics of the system, we make the following assumptions:

A1 Each site is modified independently of the state of other sites.
A2 The rates of modification are identical across all sites.

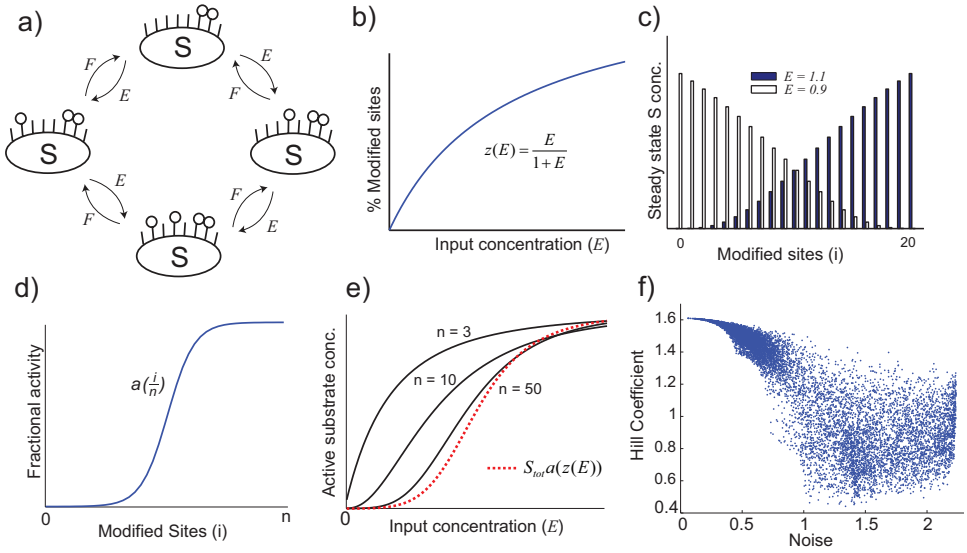

Fig. 1 **a:** A nonsequential, multisite modification system. The substrate S is modified at a linear rate proportional to the concentration of the modifying enzyme E at every site. Here, the arrows indicate irreversible chemical reactions. **b:** The overall fraction of modified sites in the sample as a function of E. **c:** Steady state distribution of the substrate S_i with exactly i modified sites in the nonsequential case, for $n = 20$, $F = 1$, and $E = 0.9$, $E = 1.1$. **d:** The activity of the substrate S_i, $i = 1 \dots n$, using the fractional activity function $a(x) = \frac{x^6}{0.5^6+x^6}$. **e:** Dose response function of the substrate activation with 3, 10, and 50 sites. The function $S_{tot}a(z(E))$ approximates f for large values of n. **f:** Apparent Hill coefficient of a nonsequential system with $n = 6$ sites and site parameters $k_1, \dots, k_6$, for 10,000 randomly chosen values of the k_i. The noise is the standard deviation of the k_i divided by their mean.

A3 The activation level of the protein depends only on the number of modified sites.

Thus if a substrate in state S_I is not yet modified at site i, the modification at this site takes place at a rate $\alpha E \cdot S_I$. If S_I is already modified at site i, then this modification is removed at a rate $\beta F \cdot S_I$. For simplicity we set here $\alpha = \beta = F = 1$. Notice that A1 rules out any type of direct or indirect cooperative behavior at the level of site modification.

Suppose that $z_i(E)$ is the fraction of protein with the i-th site modified at steady state. By A2, this fraction should not depend on i, so we can drop the subscript and simply refer to $z(E)$. This can be interpreted as the overall fraction of modified sites in the sample, or the probability that a randomly chosen site in a random protein is modified. Using the independence assumption one can derive much information about the different conformations of the protein itself from $z = z(E)$. For example, suppose $n = 3$ and S_{101} is the concentration of protein with exactly the first and last sites modified. Then $S_{101}/S_{tot} = z(1-z)z$, since the probability that a randomly chosen protein is

in that state is equal to the product of the probabilities of the three independent events.

Define S_i as the concentration of protein at steady state that has exactly i modified sites. Then the site independence assumption can be used to calculate

$$\frac{S_i}{S_{tot}} = \binom{n}{i} z^i (1-z)^{n-i},$$

where $z = z(E)$. Now suppose that the activity of a protein S_i is $a(i/n)$, using the fractional activity $a(x)$. The total protein activity is

$$f(E) = \sum_{i=0}^{n} a(i/n) S_i.$$

One can expand as

$$\frac{f(E)}{S_{tot}} = \sum_{i=0}^{n} a(i/n) \frac{S_i}{S_{tot}} = \sum_{i=0}^{n} a\,(i/n) \binom{n}{i} z^i (1-z)^{n-i}, \tag{2}$$

for $z = z(E)$. If we view z as an independent variable, then the right hand side of (2) belongs to a family of functions known as Bernstein polynomials [4,19, 34]. It is shown in the references that if a is any continuous function, then the right hand side of (2) converges towards $a(z)$ as $n \to \infty$.

We use this approximation to simplify the formula for $f(E)$ and conclude that for large values of n,

$$f(E) \approx S_{tot} a(z(E)). \tag{3}$$

Equation (3) is interesting because it directly relates three different quantities that can be measured experimentally: the fraction $z(E)$ of modified sites for a given input E, the relative activity $a(x)$ of S given a fraction x of modified sites, and the overall dose response for given E.

This argument was carried out for any function $z(E)$. To be more concrete, one can model the dynamics of the individual sites using the simple reaction

$$\mathrm{A_i} \underset{\beta F}{\overset{\alpha E}{\rightleftharpoons}} \mathrm{B_i},$$

where A_i is the concentration of S with i-th site unmodified and B_i is the concentration of S with a modified i-th site. One can easily compute the concentration of $z(E)$ at steady state,

$$z(E) = \frac{E}{F\beta/\alpha + E}.$$

Using this simple linear reaction for activation and inactivation, the model is essentially equivalent to the Adair model of ligand binding for $K_i = 1$, $i = 1 \dots n$. See the recent review [10] for a derivation and the classical reference [6].

The function $z(E)$ is displayed in Figure 1b for $F\alpha/\beta = 1$, and the steady state distribution of the S_i in the case $n = 20$ and $E = 0.9$, $E = 1.1$ can be seen in Figure 1c. Using the fractional activity displayed in Figure 1d, the dose responses for different values of n are shown in Figure 1e along with the limiting function $S_{tot}a(z(E))$. The definition of the fractional activity function (Figure 1d) has some similarity with an experimental measurement in [31], where the authors consider the conformational change of hemoglobin as a function of fractional oxygenation.

A common quantitative measure of the ultrasensitivity of a dose response curve f is the *apparent Hill coefficient* [14] and defined by

$$H = \frac{\ln 81}{\ln \frac{EC90_f}{EC10_f}},$$

where $EC10$ and $EC90$ are the inputs that generate 10% and 90% of the response (Figure 2d). In the special case of Hill functions $f(x) = x^h/(K^h+x^h)$ this is, somewhat surprisingly, the same value as the Hill coefficient h. In that sense the apparent Hill coefficient H can be thought of as a generalization of the measure h used for Hill functions.

Recall that Assumption A2 states that the different sites have identical modification dynamics. In Figure 1f we include a computation of the apparent Hill coefficient H for a nonsequential system with $n = 6$ sites, where the rates of modification vary from site to site. Specifically, if a phosphoform S_I is not yet modified at site i, the modification at this site takes place at a rate $\alpha_i E \cdot S_I$. If S_I is already modified at site i, then the site is removed at a rate $\beta_i F \cdot S_I$. At steady state the dynamics only depends on the dissociation constant $k_i = \frac{\beta_i F}{\alpha_i}$. We randomized the values of the k_i 10,000 times and plotted H as a function of the noise i.e. the standard deviation of the k_i divided by their mean. Half of the 10,000 parameter sets were chosen from an exponential distribution and half from a uniform distribution over the range 10^{-2} to 10^3. One can see that maximum ultrasensitivity is attained when the noise is minimal i.e. when the site parameters are all equal. A more detailed exploration of parameter variability in this system will be discussed in a future paper by the authors [35].

Since no assumptions were made about the form of the function $z(E)$ in the derivation of equation (3), one can replace the linear kinetics with a more complex Michaelis-Menten kinetics for the separate modification and de-modification reactions. This could lead to a more realistic form for the function $z(E)$, and it can allow to enhance this mechanism with zero-order effects [14].

Regarding the fractional activity $a(x)$, it is common in the literature to assume that the only active protein is S_n (see eg [16]). In previous work including one of the authors [42], a value $\bar{k}$ is introduced so that S_i is fully active for $i \geq \bar{k}$ and fully inactive for $i < \bar{k}$. An arbitrary fractional activity $a(x)$ generalizes both of these scenarios.

3 Unlimited ultrasensitivity in sequential systems

Consider a substrate molecule S with n modification sites, which is modified in a *sequential* manner by a protein E, and which loses these modifications through the action of the protein F. Each of these reactions is assumed to be irreversible, however they can involve covalent or non-covalent modifications. We let F be constant in the analysis and explore how the activity of S changes as the concentration of E increases. The variables S_i denote the concentration of the substrate that has exactly i modified sites, $i = 0, \dots, n$. A sample distribution of this system at steady state is shown in Figure 2b for $n = 20$ and E slightly larger or smaller than F. Once again we use the fractional activity function $a(x)$ to describe the activation of a given substrate molecule, that is, we suppose that the level of activity of S_i is $a(\frac{i}{n})$. The dose response of the system is defined as

$$f(E) = \sum_{i=0}^{n} a\left(\frac{i}{n}\right) S_i.$$

Using the fractional activity $a(x) = \frac{x}{1+x}$, Figure 2d shows the associated dose responses for various values of n. Even though $a(x)$ is not ultrasensitive, the active protein concentration $f(E)$ can become quite ultrasensitive as a function of the input E.

Through a series of approximations we derive an estimate of the coefficient H of the dose response in a sequential system, for an arbitrary fractional activity $a(x)$. Surprisingly, we find that H satisfies the formula

$$H \approx const.(n+1),$$

i.e. it increases roughly linearly with $n + 1$. As an alternative to the mathematical analysis, one can compute H_f numerically for different values of n (Figure 2e). The simulation validates the estimate since it closely resembles a straight line $\frac{1}{2}(n+1)$, for n around 6 or larger. This generalizes in an important way the recent work by one of the authors in [42].

We model the system linearly using the network illustrated in Figure 2a, that is

$$\frac{dS_i}{dt} = \alpha E \cdot S_{i-1} - \beta F \cdot S_i + \beta F \cdot S_{i+1} - \alpha E \cdot S_i, \quad 0 < i < n, \tag{4}$$

and similarly for $i = 0, n$. Also, we assume that $\alpha = \beta = F = 1$ (otherwise one can replace E below by $u = \frac{\alpha E}{\beta F}$).

At steady state, $E \cdot S_i = S_{i+1}$ for each i; this can be shown first for $i = 0$, and then for larger i by induction. Therefore $S_i = E \cdot S_{i-1} = E^2 \cdot S_{i-2} = \ldots = E^i \cdot S_0$, the total protein concentration can be written as $S_{tot} = \sum_{i=0}^{n} E^i \cdot S_0$,

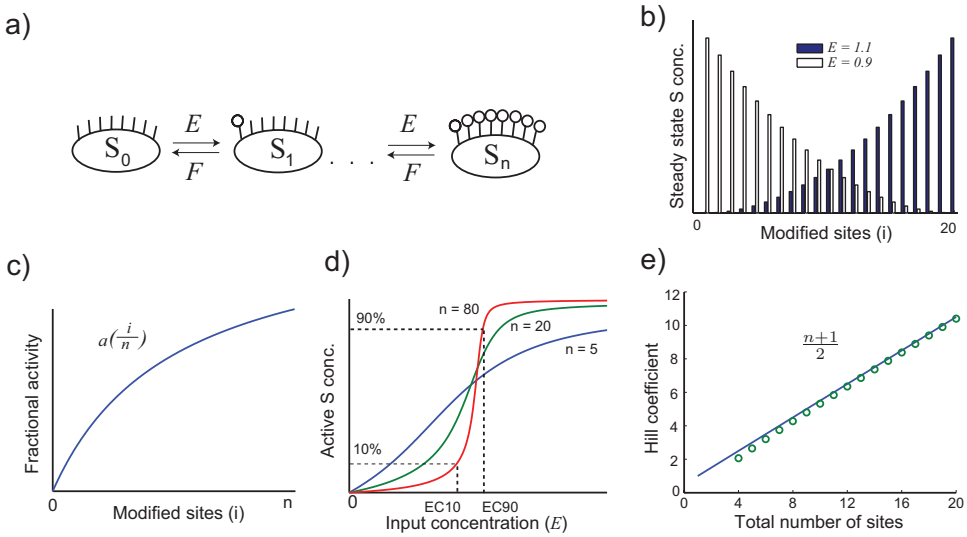

Fig. 2 **a:** A sequential modification system for a substrate protein with n sites. The arrows indicate irreversible chemical reactions using a linear or Michaelis-Menten framework. **b:** Steady state distribution of the substrate S for $n = 20$ and $F = 1$, using two different values of the input E. **c:** Fractional activity of the substrate S_i (on a scale from 0 to 1) as a function of i, using the base function $a(x) = x/(1 + x)$. **d:** Dose response function for the substrate with the fractional activity given in Figure 2c. As the number of sites increases, the dose response becomes more switch-like. The definition of EC10 and EC90 is also shown, used for the definition of the apparent Hill coefficient H. **e:** Numerical calculation of the apparent Hill coefficient of the dose response for different values of the number of sites.

and $S_i = S_{tot}E^i / \sum_{i=0}^{n} E^i$. The active protein concentration is

$$f(E) = \sum_{i=0}^{n} a\left(\frac{i}{n}\right) S_i = S_{tot} \frac{a(\frac{0}{n}) + a(\frac{1}{n})E + a(\frac{2}{n})E^2 + \ldots + a(\frac{n}{n})E^n}{1 + E + \ldots + E^n}. \quad (5)$$

As it turns out, there is a simple approximation of $f(E)$ that allows to estimate H_f for arbitrary $a(x)$. The denominator of $f(E)$ can be approximated by the integral

$$1 + E + \ldots + E^n \approx \int_0^{n+1} E^x dx.$$

One can make a similar approximation for the numerator, namely

$$a\left(\frac{0}{n}\right) E^0 + \ldots + a\left(\frac{n}{n}\right) E^n \approx \int_0^{n+1} a\left(\frac{x}{n}\right) E^x dx.$$

It should be noted that in the above integral $a(x)$ is evaluated at the point $\frac{n+1}{n} > 1$; however a is only defined on $[0, 1]$. One can resolve this issue by

simply redefining a such that $a(x) = a(1)$ whenever $x > 1$. Therefore

$$f(E) \approx S_{tot} \frac{\int_0^{n+1} a(\frac{x}{n}) E^x dx}{\int_0^{n+1} E^x dx}.$$

Now consider the function g defined by

$$g(\alpha) = \frac{\int_0^1 a(y) e^{\alpha y} dy}{\int_0^1 e^{\alpha y} dy}.$$

Making the change of variables $y = \frac{x}{n+1}$ in the approximation of $f(E)$,

$$\begin{aligned} f(E) \approx S_{tot} \frac{\int_0^1 a(\frac{n+1}{n} y) E^{(n+1)y} dy}{\int_0^1 E^{(n+1)y} dy} &\approx S_{tot} \frac{\int_0^1 a(y) E^{(n+1)y} dy}{\int_0^1 E^{(n+1)y} dy} \\ &= S_{tot} g((n+1) \log E). \end{aligned}$$

For the function $g(\alpha)$, $p = EC10_g$ and $q = EC90_g$ are well defined, since $g(\alpha)$ is a continuous, monotone function approaching $a(0)$ for $\alpha \to -\infty$ and $a(1)$ for $\alpha \to \infty$; it is only necessary to satisfy $a(0) \leq 0.1a(1)$. Since g is not a function of n, both p and q are independent of n.

Then $e^{\frac{p}{n+1}} \approx EC10_f$, since

$$f(e^{\frac{p}{n+1}}) \approx S_{tot} g((n+1) \ln e^{\frac{p}{n+1}}) = S_{tot} g(p) = 0.1 g_{max} S_{tot} = 0.1 f_{max}.$$

Likewise, $e^{\frac{q}{n+1}} \approx EC90_f$. The Hill Coefficient of f is therefore

$$H_f = \frac{\ln 81}{\ln \frac{EC90_f}{EC10_f}} \approx \frac{\ln 81}{\ln \frac{e^{\frac{q}{n+1}}}{e^{\frac{p}{n+1}}}} = \frac{\ln 81}{q-p}(n+1).$$

In other words, if $a(x)$ is an arbitrary monotone increasing fractional activity (such that $a(0) \leq 0.1a(1)$) then H_f *is roughly proportional to* $n+1$.

If $a(x)$ is a decreasing function on [0,1] such that $a(1) < 0.1a(0)$, then one can follow a very similar argument. This represents the case when the substrate S is inactivated (rather than activated) by the modifications. In this case, one can adapt the definition of the apparent Hill coefficient as $H = \frac{\ln 81}{\ln \frac{EC10}{EC90}}$.

When each modification reaction is modeled using the Michaelis-Menten framework rather than linear kinetics, the dose response curve in fact retains the same form (5), with the caveat that E represents the unbound kinase in the system, rather than the total kinase; for a derivation see [16,42]. Also, if the K_m constant of the enzymatic reactions is large, then the reaction rates can be approximated with linear terms, reducing the dose response to this same equation [5]. Any of these two alternative arguments can be used to approximate H in the form derived above.

4 Ultrasensitivity in the yeast pheromone pathway

We illustrate these ideas in a model of the ultrasensitive shutdown of the pheromone pathway by the cell cycle regulator Cdk1 in budding yeast, based on a model by Serber and Ferrell under somewhat different assumptions [36]. Haploid yeast cells belong to one of two different mating types, so-called a and α, which carry out a form of sexual reproduction. The a cells only respond to the reproductive pheromones of the α cells, and similarly the α cells only respond sexually to the pheromones released by a cells. During mating the two haploid cells fuse into a single diploid cell, which then begins to bud and form a colony [2].

Another alternative that haploid cells have for reproduction is through haploid budding i.e. by forming a haploid daughter cell through mitosis. Yeast cells ensure that mating and haploid budding don't take place simultaneously in the same cell, since they are incompatible physiological processes. They ensure this by shutting down the pheromone pathway when they are undergoing mitosis.

The protein Ste5 plays an important role in the pheromone MAPK pathway. In its dephosphorylated state, it binds to the cell membrane upon ligand binding near the pheromone receptors and their associated heterotrimeric G proteins [8,33] (Figure 3a). In this bound state Ste5 acts as a scaffold for the activation by membrane-bound Ste20 of the three proteins Ste11, Ste7, and Fus3, and it permits the transduction of the pheromone signal. However, Ste5 can be phosphorylated on any of eight phosphorylation sites by cyclin dependent kinases (CDKs) that regulate the cell cycle. When Ste5 is fully phosphorylated, it cannot bind to the membrane and signal transduction is prevented (Strickfaden et al. [39]). In this sense, one can say that Ste5 is active when bound to the membrane and inactive when unbound from it.

This system provides a good framework for the model in the nonsequential case. Here Ste5 is the multisite substrate with $n = 8$, and modifications are in this case phosphorylations by the Cdk1 kinase. The phosphorylations are eliminated by an unspecified phosphatase F such as PP2A. The fractional activity $a(x)$ can be simply interpreted as the fraction of time a Ste5 molecule spends bound to the cell membrane, given that it has a fraction x of phosphorylated sites. It is a monotonically decreasing function.

Strickfaden et al. explore, through site-directed mutagenesis of the eight individual sites, which of them need to be phosphorylated in order to effectively shut down the pheromone pathway. They find that none of them are necessary by themselves, but that it is rather the collective effect of several phosphorylations that causes Ste5 to become inactive. This points towards a bulk electrostatic behavior for this system, and it provides evidence for assumption A3. Furthermore they find that while the kinase "could inhibit signaling to a measurable degree when Ste5 retained four or five sites, inhibition was much stronger when Ste5 retained six, seven, or eight CDK sites" [39]. We incorporate this information into the fractional activity $a(i/n)$ and assume

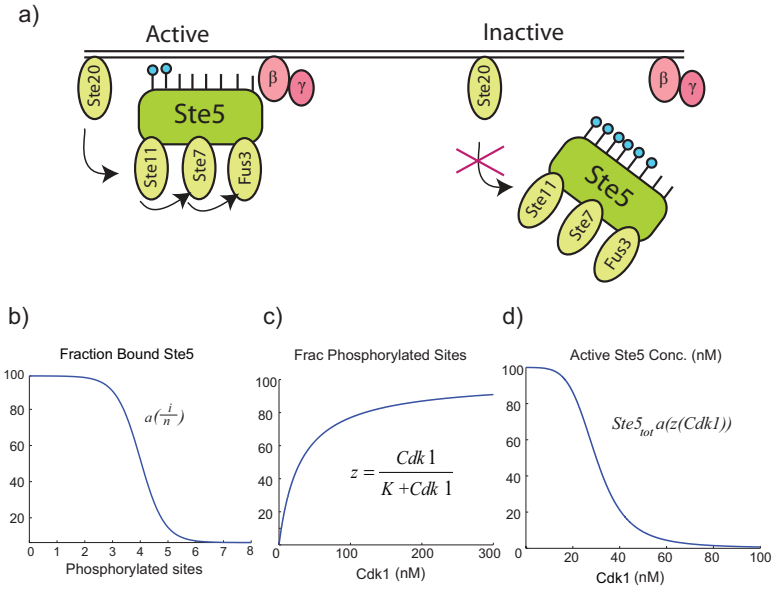

Fig. 3 a: The Ste5 scaffold must be bound to the cell membrane in order to relay the pheromone pathway signal downstream. The rate of dissociation of Ste5 from the cell membrane increases with the number of phosphorylations. In contrast to Figure 1, here the arrows indicate general activation rather than a specific chemical reaction step. **b:** The fraction of Ste5 bound to the membrane (i.e. active) as a function of the number of phosphorylated sites. The half maximal activation of Ste5 takes place at $i = 4$. **c:** Overall fraction z of phosphorylated Ste5 sites as a function of Cdk1 concentration. **d:** Nonsequential model of Ste5 activity dose response as a function of its kinase Cdk1.

that half-maximal inhibition of Ste5 takes place with four phosphorylations, i.e. $a(1/2) = a(4/8) = 0.5$ (Figure 3b).

We calculate the fraction of modified sites $z(Cdk1)$ as a simple Michaelis-Menten curve $Cdk1/(K + Cdk1)$ (Figure 3c). Then the dose response curve of Ste5 can be plotted as a decreasing function of Cdk1 (Figure 3d). This analysis is very similar to that carried out in [36], but the authors in that paper assume that Ste5 is phosphorylated differently on and off the membrane, which would actually violate our assumption of independence (see the Discussion). In the context of that paper, it is shown here that the system can be ultrasensitive without making that assumption, as long as the dissociation rate of Ste5 increases exponentially with the number of phosphorylations.

Notice that Ste5 has also been described as a key protein in the ultrasensitive activation of the pheromone pathway, as a function of pheromone concentration [27]. This is a similar but different process from the shut-down of the pathway as a function of Cdk1 kinase during cell division.

Parameter Values We set Ste5_{tot}=100 nM, i.e. 2000 Ste5 molecules per cell according to the Yeast GFP Fusion Localization Database [13] based on a usable cytosolic cell volume of 30 femtoliters. A similar analysis yields a max-

imum active Cdk1 concentration of around 300 nM, and we set the $EC50$ of the function $z(Cdk1)$ as $K = 30$ nM. The fractional activity $a(x)$ was derived as described below in Section 6, using the parameters $K_{d,50} = 1nM$, $c = 2.3$ [39].

5 Ultrasensitivity and adaptation in bacterial chemotaxis

E. coli and other bacteria move in search of food by rotating whip-like appendages called flagella. The bacterium controls its direction of movement by regulating the orientation in which the flagellum rotates. When the flagella rotate counterclockwise, they bundle together and form a tail that propels the bacterium to run in one direction. When the bacterium is searching for a new direction of motion, it does this by rotating the flagella in the clockwise direction. This causes the bacterium to tumble and rotate randomly around. An *E. coli* bacterium has about half a dozen flagella and alternates between clockwise and counterclockwise rotation to create a biased random walk. See Baker et al. and Wadhams et al. [1,41] for reviews of the signal transduction of bacterial chemotaxis, and Tindall et al. [40] for a review of models of chemotaxis at the cellular level.

The direction in which the flagella rotate is controlled by the flagellar motor, which is in turn regulated by the chemotaxis pathway. When few ligands are bound to chemoattractant receptors, the portion of the receptor inside the cell activates the protein CheA through phosphorylation. When CheA is activated, it phosphorylates the protein CheY, which interacts with the flagellar motor and sends the signal to rotate clockwise, causing the tumbling motion (Figure 4a). Importantly, some time after the ligand is bound the cell *adapts* to this ligand concentration as a new normal and returns to tumbling mode. In this way, the cell will only continue to run as long as the ligand concentration continues to increase, and it will likely tumble otherwise before finding a new random direction.

In the current framework, one can think of n receptors bound into a tightly interconnected receptor complex including several copies of CheA and the adaptor CheW (not included in the model). The receptor affinity to chemoattractant is essentially unchanged regardless of the state of the system, and the ligands bind independently of each other. However the strong interactions within the complex ensure that all CheA molecules share a similar level of activity, which decreases in an ultrasensitive way as the fraction of bound ligands increases.

As before, define $z(L) = L/(K_d + L)$, the probability that a random receptor monomer is bound to the ligand. Also suppose that $a_M(x)$ represents the overall fractional activity of the receptor complex, given a fraction x of bound ligands. This activity depends on the average level of methylation in the receptors, $M \leq M_{max}$. Using the argument in Section 2 for nonsequential systems, one can deduce that the fractional activity of the complex approximates $a_M(z(L))$ for large m. The equations of the model are defined by

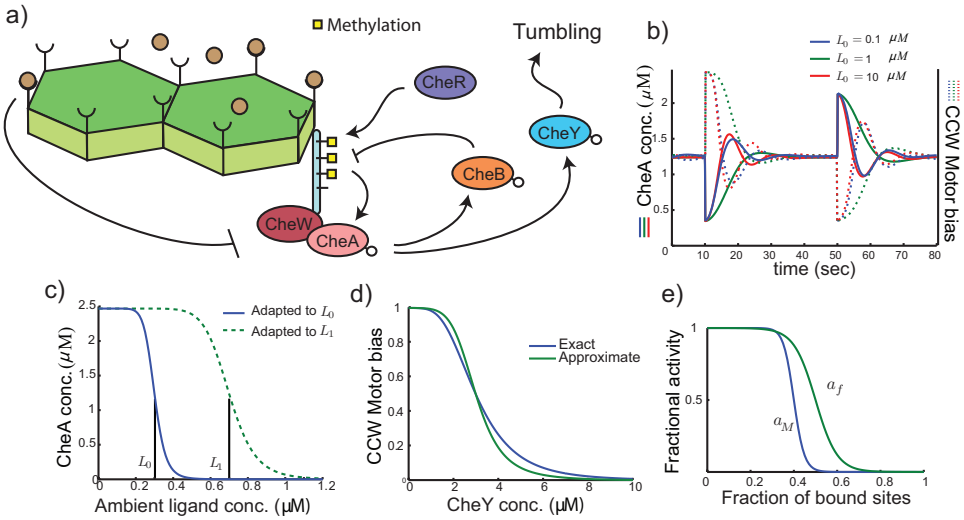

Fig. 4 **a:** Graphical representation of the chemotaxis pathway. A chemoattractant L binds to an array of receptors, triggering a chain of reactions that makes the cell more likely to run than to tumble. The arrows loosely symbolize activation (arrow head) or inhibition (flat head). **b:** Timecourse after stimulation with a ligand concentration that increases by 20% at $10s$ and then decreases to its original value at $50s$. **c:** Short term dose response of CheA activity under a ligand concentration L shortly after the cell has been exposed for a prolonged period to a concentration L_0 (blue, solid) or L_1 (dashed, green). The dose response is therefore ultrasensitive in the short term and adaptive in the long term. **d:** Comparison of the exact dose response and the approximation $S_{tot}a_f(z(Y))$ for the motor bias system under increasing CheY concentration. **e:** The fractional activity $a_M(x)$ of the receptor array given a fraction x of bound ligands, and the propensity of the flagellum for counterclockwise motion given a fraction x of CheY-bound sites ($a_f(x)$).

$$
\begin{aligned}
A' &= V_{max} a_M(z(L)) - (k_{ay} + k_{ab})A \\
B' &= k_{ab}A - k_{bb}B \\
Y' &= k_{ay}A - k_{-y}Y \\
\frac{1}{\epsilon}M' &= k_m R - k_{-m}B,
\end{aligned}
$$

using the fractional activity

$$
a_M(x) = \frac{\gamma(M)^p}{(\frac{x}{x-1})^p + \gamma(M)^p}.
$$

Here A, B, Y, and R represent active CheA, CheB, CheY, and CheR respectively, and the function $\gamma(x) := x/(M_{max} - x)$ is the inverse of the Michaelis-Menten function $M_{max}x/(1 + x)$.

In Figure 4b, the simulation shows the CheA response to a 20% increase in ligand concentration at $t = 10$ seconds, followed by the reduction to baseline concentration at $t = 50$ seconds. The baseline ligand concentrations are $L_0 = 100\ nM$, $L_0 = 1\ \mu M$, and $L_0 = 10\mu M$, a 100-fold range. Notice that the system starts at the same steady state CheA concentration in all three cases, and that it adapts to this concentration after a transient response.

After the system has adapted to an ambient ligand concentration L_0, it is highly sensitive to short term changes in ligand concentration, as shown in Figure 4c. Moreover, if the ambient ligand concentration is changed for a longer period of time to L_1, the system adapts and becomes again ultrasensitive to short term changes in the concentration (Figure 4c, dotted line). The key to the adaptation is the fact that the methylation reactions are slower than CheY activation and inactivation. This is shown in the model by the $1/\epsilon$ term for the methylation equation. See below for a precise analysis of this system. The shape and apparent Hill coefficient of the graphs in Figure 4c are consistent with experimental data measured by Sourjik and Berg [37].

Notice that the rates of enzymatic activation do not depend on the substrate concentration. This can be the result of a small K_m for the enzymatic reactions, leading to an essentially constant maximal rate of activation. The transfer of the phosphate from CheA to CheB and CheY is explicitly included, and methylation has the effect of changing the rate of CheA activation without altering the ligand binding rates. While L can take arbitrarily large values, methylation levels are bounded by M_{max}.

The function $a_M(x)$ decreases with x and increases with M, in fact it resembles a decreasing Hill function. For fixed M, the EC50 of this equation is x such that $\gamma(M) = x/(1 - x)$, that is $EC50_{h_M} = \gamma(M)/(1 + \gamma(M))$. This fractional activity only depends on the parameter M_{max}, and it is plotted for a sample value of M in Figure 4d. One can also show with a simple calculation that in fact

$$a_M(z(L)) = \frac{\gamma(M)^p}{(L/K_d)^p + \gamma(M)^p}.$$

Analysis of Adaptation: Fix the ligand at a concentration $L = L_0$ in order to study the system at steady state. It is easy to show that

$$A = \frac{k_{bb}}{k_{ab}}B = \frac{k_{bb}}{k_{ab}}\frac{k_m}{k_{-m}}R$$

regardless of the input L_0 (notice that CheR is a parameter in this system). This proves the adaptation property of the model at steady state. In order to compute the steady state value of M, calculate

$$A = \frac{V_{max}}{k_{ay} + k_{ab}} \frac{\gamma(M)^p}{L_0^p + \gamma(M)^p},$$

so that

$$\frac{\gamma(M)^p}{(L_0/K_d)^p + \gamma(M)^p} = \frac{k_{ay} + k_{ab}}{V_{max}} \frac{k_{bb}}{k_{ab}} \frac{k_m}{k_{-m}} R.$$

Calibrate the system by requiring that the right hand side be equal to 0.5, that is

$$\frac{k_{ay} + k_{ab}}{V_{max}} \frac{k_{bb}}{k_{ab}} \frac{k_m}{k_{-m}} R = \frac{1}{2}, \tag{6}$$

in which case one can deduce $\gamma(M) = L_0/K_d$ or $M = M_{max} L_0/(K_d + L_0)$. In this way the methylation grows at steady state to compensate for any increase in the ligand concentration.

Analysis of Sensitivity: If the ligand concentration is quickly changed by a factor of δ from L_0 to $L = \delta L_0$ after adaptation has taken place, one can approximate $M' = 0$ and allow the resulting equations to converge to steady state. Define $\Gamma_1 := \frac{V_{max}}{k_{ay}+k_{ab}}$. Then since $\gamma(M) = L_0/K_d$,

$$A = \Gamma_1 \frac{(L_0/K_d)^p}{(L/K_d)^p + (L_0/K_d)^p} = \Gamma_1 \frac{L_0^p}{\delta^p L_0^p + L_0^p} = \Gamma_1 \frac{1}{\delta^p + 1}.$$

In this way CheA changes in the short term in an ultrasensitive manner that does not depend on the original ligand concentration L_0. This also explains the Hill function shape of the graphs in Figure 4c.

Flagellar Motor Activation One can also examine the ultrasensitive behavior of the flagellar motor as a function of ligand concentration. The flagellar motor has a ring with around $m = 40$ copies of the FliM protein, which have an affinity to active CheY and are believed to influence the orientation of the motor [9]. Define the motor bias as the fraction of time that the motor spends in clockwise orientation.

It is unclear how the FliM proteins influence flagellar motor orientation. However consider a situation, perhaps based on bulk electrostatics, where 15 or fewer CheY-bound sites are virtually guaranteed to keep the system in counterclockwise rotation, while 25 or more bound sites virtually guarantee clockwise rotation. Under such a scenario, even uncooperative binding of CheY to independent FliM molecules would lead to an ultrasensitive response by the framework in this paper.

Using a nonsequential model for CheY binding to the rotor, define $a_f(x)$ as the motor bias given a fraction x of FliM proteins bound to CheY (Figure 4e). We will assume that $a_f(x)$ is ultrasensitive as described above. As done elsewhere in the literature eg [9], set the CheY-FliM dissociation constant K_d^y to be equal to the steady state CheY concentration, i.e. $K_d^y = 3\ \mu M$. Also suppose for simplicity that the bias is 0.5 for that CheY concentration. Given

a variation of the CheY concentration Y away from steady state, the probability that a FliM site is bound at a given time is around $x(Y) = Y/(K_d^y + Y)$. Notice that this assumes the binding and unbinding of CheY is relatively fast compared to the timescale of CheY dynamics. Using the binomial formula and the bias function a_f one can compute the overall motor bias as a function of Y and estimate it from (3) to be around $a_f(x(Y))$. If a_f is an ultrasensitive function, then so is the dose response too.

The timecourse of flagellar motor bias after ligand stimulation is also shown in Figure 4b, and it confirms that the ultrasensitive behavior at the flagella enhances the response to small changes in ligand concentration.

The ultrasensitive dose response of the motor bias as a function of CheY concentration is calculated in Figure 4d. Here $H = 4.7$ using the current parameters, which is consistent with the values measured in [9]. Also displayed in this graph is the original dose response in blue, for comparison with the approximation $a_f(z(Y))$.

Model Parameters The parameters used in this model are described in Table 1. In order to fit the parameter p in the fractional activity $a_M(x)$, notice that p is the coefficient H of the short term response. This was measured experimentally by Sourjik and Berg [37], and the value $p = 10$ is in the upper range of those measurements.

Parameter	Variable	Value	Literature	
Aspartate to Tar dissociation rate	K_d	1 μM	$K_d = 1$ μM	[38]
Phosphotransfer from CheA to CheY	k_{ay}	240 s^{-1}	$k_y T = 240$ s^{-1}	[38]
Phosphotransfer from CheA to CheB	k_{ab}	3 s^{-1}	$k_b T = 6.4$ s^{-1}	[38]
Autodephosphorylation of CheB	k_{bb}	0.35 s^{-1}	$k_{-b} = 0.35$ s^{-1}	[38]
Methylation	k_m	0.08 s^{-1}	$k_{1c} = 0.17$ s^{-1}	[38]
Demethylation	k_{-m}	0.024 s^{-1}	$k_{-1} T = 0.24 s^{-1}$	[38]
Dephosphorylation of CheY	k_{-y}	100 s^{-1}	$k_{-y} Z = 20$ s^{-1}	[38]
CheR concentration	R	3.2 μM	0.3 μM	[38]
Hill coefficient of short term response	p	10	10	[37]
CheY to FliM dissociation rate	K_d^y	3 μM	3 μM	[9]
Maximum activation rate of CheA	V_{max}	600 $\mu M^{-1} s^{-1}$	n/a	
Maximum methylation state	M_{max}	5 sites	5 sites	[40]
Time scale decomposition constant	ϵ	0.2	n/a	

Table 1 Parameter values used in the chemotaxis model. In the right column the corresponding parameters in the literature are described. In the case of Spiro et al. [38], we use the notation in that reference (T=Tar, Z=CheZ). The critical ultrasensitivity parameter p was measured directly in experiments by Sourjik and Berg [37].

The reaction rates $k_{ay}, k_{ab}, k_{bb}, k_m, k_{-m}, k_{-y}$ and K_d are taken from the chemotaxis model by Spiro et al. [38]. Most of these rates belong to second order reactions in Spiro et al., in which case they were multiplied by the

respective substrate concentration to use them in first order reaction terms. The parameters from Spiro et al. seem to affect the steady state of the system only in aggregation, and therefore their individual values are not as important. For instance, for the steady state only their product in equation (6) is relevant. The value $R = 3.2\ \mu M$ was chosen to calibrate (6). The parameters of the equation for M' were rescaled by the use of $\epsilon = 0.2$, and the maximum CheA activation rate was set at $V_{max} = 600 M^{-1} s^{-1}$. The parameter $M_{max} = 5$ is the number of methylation sites in Tar, the most common chemotaxis receptor protein [40]. $K_d^y = 3\ \mu M$ is the average concentration of CheY after adaptation [9], and it also the steady state CheY concentration in the model.

6 Ultrasensitive fractional activity functions

Since this framework for ultrasensitive dose responses is dependent on the ultrasensitive behavior of the fractional activity function $a(x)$ (at least in the nonsequential case), in this section we argue that there are several mechanisms to create such ultrasensitive functions. This problem has also been studied in the literature, for instance Lenz and Swain developed a entropy argument in the case of disordered proteins with multiple phosphorylation sites [24].

As an important special case, suppose that there are two distinct states for the substrate, an active state A and an inactive state I, and that each modification decreases (or raises) the energy of the active state by a fixed amount. The transitions between the active and inactive states can be described by

$$\mathrm{I} \underset{\beta}{\overset{\alpha}{\rightleftharpoons}} \mathrm{A},$$

with rates of transition α and β. At steady state, one can define the activity as the likelihood that the substrate is active, namely $1/(1 + K_d)$ for $K_d = \beta/\alpha$. Given the assumption on the modifications, a direct application of the Boltzmann distribution is that K_d depends exponentially on i, the number of modified sites [3,36]. Set $K_d = K_{d,50} e^{c(i-n/2)}$ for some constants $K_{d,50}$ and c. The $n/2$ in this expression is included so that for $i = n/2$, $K_d = K_{d,50}$ has a fixed value regardless of n. If $x = i/n$ is the fraction of modified sites, then

$$a(x) = \frac{1}{1 + K_d} = \frac{1}{1 + K_{d,50} e^{c(i-n/2)}} = \frac{1}{1 + K_{d,50} e^{cn(x-\frac{1}{2})}}. \tag{7}$$

For example, in the Ste5 system the active and inactive states correspond to Ste5 bound or unbound from the membrane, and each phosphorylation inhibits membrane binding (see the calculation in [36]). Setting $K_{d,50} = 1nM$, $c = 2.3$ [28,30], and $n = 8$, one obtains a system with K_d values ranging from $10^{-4}\ nM$ to $10^4\ nM$, which is within the physiological range [5]. The resulting fractional activity $a(x)$ is plotted in Figure 3b. For the CheY-FliM system in the regulation of the flagellar motor (a_f in Figure 4e), we used this same system with $K_{d,50} = 1$, $n = 40$, $c = -0.5$.

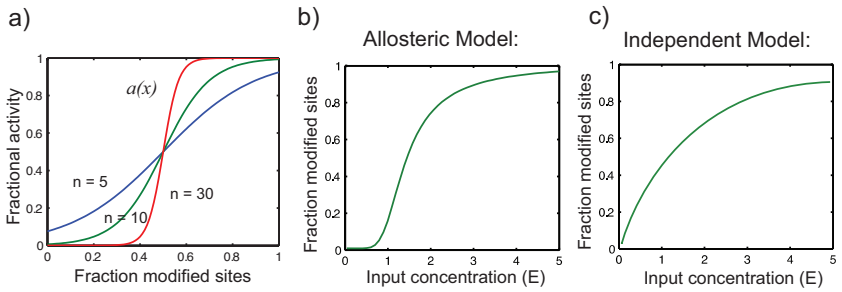

Fig. 5 **a:** The fractional activity function $a(x)$ as derived in Section 6, for increasing values of n; here $c = -1$, $K_{d,50} = 1$. **b,c:** A possible approach to differentiate experimentally between allosteric and independent multisite models with an ultrasensitive dose response. For strongly allosteric models the fraction of modifications increases in an ultrasensitive way as a function of E (b). In independent models this function need not be ultrasensitive, since the ultrasensitivity can be contributed by the fractional activity function $a(x)$ (c).

Notice in Figure 5a that this function becomes increasingly ultrasensitive for larger values of n. In fact, it is shown in Section 7 that H is approximately proportional to n, for any set of parameters. This simple mechanism is therefore sufficient to create powerful fractional activities that can lead to ultrasensitive dose responses as described in Section 2.

It is interesting that the function in (7) is actually dependent on n, unlike the fixed functions considered in the previous sections. Moreover, since $a(x)$ becomes arbitrarily ultrasensitive for increasing values of n, one can still produce increasingly ultrasensitive responses in the nonsequential case for large n.

There are several other ways to obtain an ultrasensitive fractional activity $a(x)$ depending on the biological context. For instance, there is no need to assume that there is an active and an inactive state, but rather a continuum of activity as x increases. This could be the case eg for the receptor complex in the chemotaxis example, where a more heuristic fractional activity was used. In yet another class of systems, the fractional activity $a(x)$ could be calculated through computational simulations in the absence of a mathematical formula. For example, in related ongoing work we are studying the regulation of gene expression through DNA packaging. The packaging of DNA can be controlled by the amount of acetylation present in its bound histones. Histones interact with each other and with other proteins in complex and numerous ways, and preliminary simulations based on percolation theory show that DNA can unpack in an ultrasensitive way as the fraction of acetylation increases.

7 Apparent Hill Coefficient in Equation (7)

A similar technique as used in the sequential dose response applies to the estimated activity function $a(x)$ in equation (7). One can verify $a(x) = g(n(x-0.5))$, where $g(x) = 1/(1 + K_{d,50}e^{cx})$. If $p := EC10_g$, and $q := EC90_g$, then $EC10_a = p/n + 0.5$, and $EC90_a = q/n + 0.5$. Now,

$$\frac{q/n + 0.5}{p/n + 0.5} - 1 = \frac{q/n - p/n}{p/n + 0.5} = \frac{q - p}{p + 0.5n} \approx \frac{2(q-p)}{n}.$$

Therefore $EC90_a/EC10_a \approx \frac{2(q-p)}{n} + 1$, and

$$H_a = \frac{\ln 81}{\ln \frac{EC90_a}{EC10_a}} \approx \frac{\ln 81}{\frac{2(q-p)}{n}} = n\frac{\ln 81}{2(q-p)}.$$

This expression increases linearly with n, showing how the ultrasensitive behavior of $a(x)$ increases as n grows.

8 Discussion

As it was mentioned in the introduction, most of the research in the literature on multisite systems and ultrasensitivity focuses on the effects of cooperativity and allostery, with the implicit assumption that the sites affect the rates of modification among each other. Here we shift that focus and assume that the sites interact only at the level of protein activation. To our knowledge these simple ideas have received little attention in the context of multisite ultrasensitivity, perhaps because they might be seen as conflicting with the established mechanism of cooperativity as a source of ultrasensitive behavior. However the assumption of independence has been successfully used e.g. to reduce complexity in the context of general biochemical reactions, see the work by Walter Fontana and colleagues [7,18]. Overall, there is an enormous number of multisite systems in biology that likely benefit from ultrasensitive behavior, involving all sorts of modifications such as phosphorylation, acetylation, and methylation, and different types of 'ligand' binding such as histones binding to DNA, calcium binding to intracellular molecules, etc, and where this particular set of assumptions may be applicable. Allosteric proteins tend to have a strong secondary or tertiary structure, so the assumptions described here can be especially appealing for unstructured multisite molecules.

The Ste5 system [27], and especially the chemotaxis system, have been the focus of intensive research, and this is by no means the first time that their ultrasensitivity is modeled or proposed. Every model relies on a different assumption, whether it is the saturation of the enzymes (in zero-order systems), cooperativity and allostery, etc. The proposed mechanism relies on the ultrasensitivity of the activation gradient, which is founded on general thermodynamic principles as discussed in Section 6 and which is likely satisfied in some systems but not in others. Moreover, the derivation of the key equation

(1) is new to our knowledge, and it extends to other non-allosteric models as a useful modeling tool.

One could argue that the difference between allosteric and independent models is largely technical, and that it would be very difficult to distinguish between the two models in an actual biological system. But actually a simple experiment could provide evidence for one model or another. Suppose that one measures the fraction of modified sites as a function of the input. For example, this is the standard plot of O_2 vs fractional saturation in the hemoglobin literature [6]. If this graph is ultrasensitive, it provides evidence that modifying some sites increases the rate at which other sites are modified (Figure 5b), and therefore that this is an allosteric system. However if the graph is not ultrasensitive, yet the dose response is ultrasensitive (Figure 5c), then one can suspect that another mechanism is at hand such as the one described here. This is especially the case if the fractional activity $a(x)$ is directly measured to be ultrasensitive, as was shown in the Ste5 system [39].

One important mechanism in this context is the so-called bulk electrostatic effect [36]. For instance, each phosphorylation tends to turn the protein more hydrophilic, and it does not matter much exactly which of the sites are modified as long as they lie within a general area. This can account for assumption A3 that only the number of modified sites matters in order to determine the level of activation. In the case of receptor complexes in chemotaxis, large numbers of different receptors are thought to interact together through mechanical or electrostatic interactions to activate CheA downstream, in a way that might be comparable to bulk electrostatics. While the ultrasensitivity of a nonsequential system is limited by the apparent Hill coefficient of $a(x)$, in the derivation of the function $a(x)$ for the nonsequential case we found that $a(x)$ can actually depend on n and become increasingly ultrasensitive for large n. Taking this into account, nonsequential systems can also become highly ultrasensitive for large n.

The chemotaxis system is a relatively simple proof of principle and yet it presents several important features for such models. It is highly sensitive to small short term changes in the ligand concentration, and it adapts to any fixed ligand concentration L_0. Moreover, it has a high degree of parameter robustness, since only equation (6) is required to ensure short term ultrasensitive behavior and adaptation at steady state. These properties are difficult to find together in models that incorporate the basic biology, as discussed in Tindall et al. [40]. Following the work in [43], adaptation is modeled as the result of an integral feedback mechanism incorporated in the underlying biochemistry, at the price of somewhat non-standard reaction terms that are independent of substrate concentration. The compactness of this model is also remarkable – the core of the receptor level equations could be easily reduced to two equations, one for CheA and one for M. Other multisite models usually have multiple variables representing the same substrate in different states, which is very cumbersome for practical applications. Notice that we did not need to calculate the number of receptors n, since the approximation holds for any sufficiently large n. However n can be quite large since every edge in

the hexagonal receptor arrays contains a trimer of dimers of receptors. The flagellar motor presents yet another opportunity to model the system in the discussed framework.

An interesting fractional activity to consider is $a(x) = x$, which can be used in the context of transport molecules such as hemoglobin. In that case the dose response function is none other than the so-called fractional saturation, that is, the percentage of modified sites given an input concentration. In the nonsequential case, this system is equivalent to the so-called Adair model without cooperativity [6]. In fact it is also a special case of the KNF model [22, 23] in the absence of cooperativity. The KNF model increases ultrasensitive behavior by introducing cooperativity among the different sites, while the nonsequential model in this paper increases ultrasensitivity by making $a(x)$ itself an ultrasensitive function.

Assumption A1 regarding independence among sites is generally only satisfied as an approximation. For instance, independence is violated if the activation state of the protein has an effect on site modifications. If Ste5 is phosphorylated differently on and off the membrane (which is assumed in Serber and Ferrell [36] for this system), then multiple phosphorylations will indirectly affect additional kinase activity by de-attaching the protein from the membrane. Also consider when a full Michaelis-Menten mechanism is used as a model of site modification instead of the linear reaction rates. As the enzyme binds to its docking site, it raises the likelihood that any site becomes modified, and it cannot simultaneously modify multiple sites. This introduces positive and negative correlations in the dynamics between different sites, potentially violating independence.

Even in the face of these issues, the assumption of independence can be approximately satisfied and used leading to useful predictions. For instance, regarding the detailed balance principle, one can argue that at least for larger values of n the contribution of each modification is relatively small. In this way the modification rates at the active and inactive states are similar enough that they can be considered roughly equal, in line with other approximations commonly made in biophysical models. To draw an analogy, linear enzymatic reaction rates are often used in modeling even though they are of necessity only an approximation of the actual mechanism. We also assume that the activation of the protein does not feed back into the protein modification dynamics (eg that Ste5 phosphorylation does not depend on whether it is bound to the membrane), which may be roughly satisfied in some systems and not in others. Actually such a feedback opens other opportunities for modeling and interesting dynamics, such as an increased likelihood for bistability in the presence of protein scaffolds [5].

Assumption A2 on equal dynamics across all sites is to some extent a convenience. If the different sites have different dynamics, one can still use the remaining assumptions to describe the protein behavior using n different subsystems, one for each site. This is a large improvement over having to account separately for each of the 2^n protein states. In practice, for an unstructured protein domain with one docking site for each enzyme and multiple phospho-

rylation sites, this assumption holds only approximately, since each site may have a different position with respect to the enzyme docking sites.

Acknowledgments

We would like to thank Ned Wingreen for discussions and criticism, and Uri Alon for useful comments and advice. This material is based upon work supported by the National Science Foundation under Grants Nos. DMS-1122478 and 1129008.

References

1. Baker, M., Wolanin, P., Stock, J.: Signal transduction in bacterial chemotaxis. Bioessays **28**, 9–22 (2006)
2. Bardwell, L.: A walk-through of the yeast mating pheromone response pathway. Peptides **25**(9), 1465–76 (2004)
3. Beard, D., Qian, H.: Chemical Biophysics: Quantitative Analysis of Cellular Systems. Cambridge University Press (2008)
4. Bernstein, S.: Demonstration du théorème de Weierstrass, fondée sur le calcul des probabilités. Comm. Kharkov Math. Soc. **13**, 1–2 (1912-13)
5. Chan, C., Liu, X., Wang, L., Bardwell, L., Nie, Q., Enciso, G.: Protein scaffolds can enhance the bistability of multisite phosphorylation. PLoS Comp. Biol. **8**, 1–9 (2012)
6. Cornish-Bowden, A.: Fundamentals of Enzyme Kinetics, chap. 8. Butterworth & Co. Ltd., London (1979)
7. Danos, V., Feret, J., Fontana, W., Harmer, R., Krivine, J.: Abstracting the differential semantics of rule-based models: exact and automated model reduction. Annual IEEE Symp. Logic Comp. Sci. (2010)
8. Dohlman, H.: G proteins and pheromone signaling. Annual Rev. Physiol. **64**, 129–52 (2002)
9. Duke, T., Novère, N.L., D. Bray, D.: Conformational spread in a ring of proteins: a stochastic approach to allostery. J. Mol. Biol. **308**, 541–553 (2001)
10. Enciso, G.: Multisite mechanisms for ultrasensitivity in signal transduction. In: C. Poetsche, P. Kloeden (eds.) Nonautonomous and Random Dynamical Systems in Life Sciences, Lecture Notes in Mathematical Biology. Springer Verlag (2013)
11. Ferrell, J.: Tripping the switch fantastic: how a protein kinase cascade can convert graded inputs into switch-like outputs. Trends Biochem. Sci. **21**(12), 460–466 (1996)
12. Ferrell, J.: Q&A: Cooperativity. J. Biology **8**, 53.1–53.6 (2009)
13. Ghaemmaghami, S., Huh, W., Bower, K., Howson, R., Belle, A., Dephoure, N., O'Shea, E., Weissman, J.: Global analysis of protein expression in yeast. Nature **425**, 737–741 (2003)
14. Goldbeter, A., Koshland, D.: An Amplified Sensitivity Arising from Covalent Modification in Biological Systems. Proc. Natl. Acad. Sci. USA **78**(11), 6840–6844 (1981)
15. Goldbeter, A., Koshland, D.: Ultrasensitivity in biochemical systems controlled by covalent modification: interplay between zero-order and multistep effects. Journal of Biological Chemistry **259**, 14,441–7 (1984)
16. Gunawardena, J.: Multisite protein phosphorylation makes a good threshold but can be a poor switch. Proc. Natl. Acad. Sci. USA **102**(41), 14,617–22 (2005)
17. Hansen, C., Sourjik, V., Wingreen, N.: A dynamic signaling-team model for chemotaxis receptors in *Escherichia coli*. Proc. Natl. Acad. Sci. USA **107**, 17,170–17,175 (2010)
18. Harmer, R., Danos, V., Feret, J., Krivine, J., Fontana, W.: Intrinsic information carriers in combinatorial dynamical systems. Chaos **20**, 037,108 (2010)
19. Herzog, F., Hill, J.: The Bernstein Polynomials for Discontinuous Functions. American J. Math. **68**(1), 109–124 (1946)

20. Huang, C., Ferrell, J.: Ultrasensitivity in the mitogen-activated protein kinase cascade. Proc. Natl. Acad. Sci. USA **93**, 10,078–10,083 (1996)
21. Iakoucheva, L., Radivojac, P., Brown, C., O'Connor, T., Sikes, J., Obradovic, Z., Dunker, A.: The importance of intrinsic disorder for protein phosphorylation. Nucleic Acids Res. **32**, 1037–1049 (2004)
22. Keener, J., Sneyd, J.: Mathematical Physiology. Volume I: Cellular Physiology. Springer Science+Business Media (2008)
23. Koshland, D., Nemethy, G., Filmer, D.: Comparison of experimental binding data and theoretical models in proteins containing subunits. Biochemistry **5**, 365–385 (1966)
24. Lenz, P., Swain, P.: An entropic mechanism to generate highly cooperative and specific binding from protein phosphorylations. Curr. Biol. **16**, 2150–2155 (2006)
25. Levchenko, A.: Allovalency: A case of molecular entanglement. Curr. Biol. **13**, R876–R878 (2003)
26. Liu, X., Bardwell, L., Nie, Q.: A combination of multisite phosphorylation and substrate sequestration produces switch-like responses. Biophys. J. **98**(8), 1396–1407 (2010)
27. Malleshaiah, M.K., Shahrezaei, V., Swain, P.S., Michnick, S.W.: The scaffold protein ste5 directly controls a switch-like mating decision in yeast. Nature **465**(7294), 101–015 (2010)
28. McLaughlin, S., Aderem, A.: The myristoyl-electrostatic switch: a modulator of reversible protein-membrane interactions. Trends Biochem. Sci. **20**, 272–276 (1995)
29. Monod, J., Wyman, J., Changeux, J.: On the nature of allosteric transitions: a plausible model. J. Mol. Biol. **12**, 88–118 (1965)
30. Murray, D., Hermida-Matsumoto, L., Buser, C., Tsang, J., C.T. Sigal, C., N. Ben-Tal, N., Honig, B., Resh, M., McLaughlin, S.: Electrostatics and the membrane association of Src: theory and experiment. Biochemistry **37**, 2145–2159 (1998)
31. Ogawa, S., McConnell, H.: Spin-label study of hemoglobin conformations in solution. Proc. Natl. Acad. Sci. USA **58**, 19–26 (1967)
32. O'Shaughnessy, E., Palani, S., Collins, J., Sarkar, C.: Tunable signal processing in synthetic map kinase cascades. Cell **144**, 119–131 (2011)
33. Pryciak, P., Huntress, F.: Membrane recruitment of the kinase cascade scaffold protein Ste5 by the Gbeta gamma complex underlies activation of the yeast pheromone response pathway. Genes & Development **12**(17), 2684–2697 (1998)
34. Rivlin, T.: An introduction to the approximation of functions, chap. 1. Dover Phoenix Editions, Dover Publications, NY (2003)
35. Ryerson, S., Enciso, G.: Site variability in a multisite signal transduction system. To appear
36. Serber, Z., Ferrell, J.: Tuning bulk electrostatics to regulate protein function. Cell **128**(3), 441–4 (2007)
37. Sourjik, V., Berg, H.: Functional interactions between receptors in bacterial chemotaxis. Nature **428**, 437–441 (2004)
38. Spiro, P., Parkinson, J., Othmer, H.: A model of excitation and adaptation in bacterial chemotaxis. Proc. Natl. Acad. Sci. USA **94**(14), 7263–8 (1997)
39. Strickfaden, S., Winters, M., Ben-Ari, G., Lamson, R., Tyers, M., Pryciak, P.: A mechanism for cell-cycle regulation of MAP kinase signaling in a yeast differentiation pathway. Cell **128**(3), 519–31 (2007)
40. Tindall, M., Porter, S., Maini, P., Gaglia, G., Armitage, J.: Overview of mathematical approaches used to model bacterial chemotaxis I: the single cell. Bull. Math. Biol. **70**, 1525–1569 (2008)
41. Wadhams, G., Armitage, J.: Making sense of it all: bacterial chemotaxis. Nature Reviews, Molecular Cell Biology **5**(12), 1024–37 (2004)
42. Wang, L., Nie, Q., Enciso, G.: Nonessential sites improve phosphorylation switch. Biophys. J. **99**(6), L41–3 (2010)
43. Yi, T.M., Huang, Y., Simon, M., Doyle, J.: Robust perfect adaptation in bacterial chemotaxis through integral feedback control. Proc. Natl. Acad. Sci. USA **97**(9), 4649–53 (2000)